Are there Photons? - Heterodyning Ultra Low Intensity Electromagnetic Fields

André Malz*

In exploring the true essence of electromagnetic fields, heterodyning emerges as superior to traditional detection methods. Within heterodyning, a segment of the signal operates independently of field-matter interaction, relying solely on field-field interaction. Consequently, this approach facilitates the statistical elimination of detector influence. Analysis of the gathered data unveils energy levels comparable to those of a few photons, which are fractional and may even descend below the threshold of a single photon, thus evading any quantization effects. This unequivocally falsifies the concept of photons.

Preprint Disclaimer

The experiment presented extends its apologies to the physics community for deviating from established paradigms. It encourages further repetitions until the outcomes align with conventional understanding.

I. INTRODUCTION

Figure 1 depicts a setup where the optical path of a laser beam is divided, with one path being delayed before being brought into interference with the other. When there is a very slight angle between the two paths reaching the detector, an interference pattern becomes observable on a camera when the beam is projected. This interference pattern persists even under significant attenuation of the laser beam, where only a minimal amount of energy, akin to that of a few photons, remains in the additional path length $\approx 2D$. Remarkably, the interference pattern persists even when the number of photons in that path approaches zero. The electrical field can be attenuated to exceedingly low values.

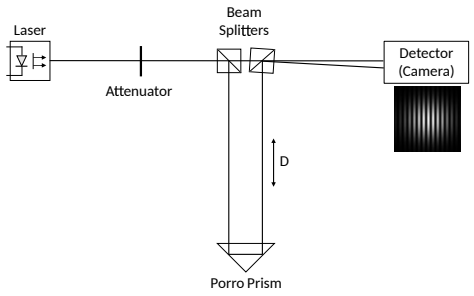

FIG. 1. Attenuated Laser, Interference

Figure 2 depicts a setup akin to the one described, focusing on the energy level of the signal beam. In this configuration, heterodyning serves as the detection scheme. The interference arises through the process of sweeping the laser frequency and subsequently recombining the attenuated laser with its non-attenuated counterpart, also called local oscillator (LO). The resulting signal is captured by a balanced detector and sampled (e.g. 500MHz). As the attenuated laser experiences a delay, the frequency discrepancy caused by the time delay induces a beat frequency in the detected signal.

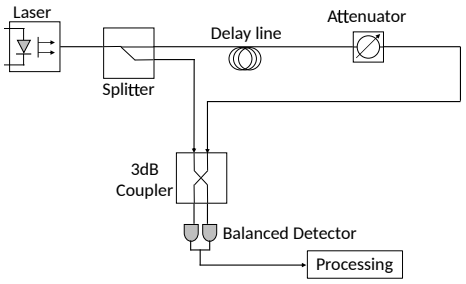

FIG. 2. Attenuated Laser, Heterodyning

In both setups, the electromagnetic field can be attenuated to ultra-low intensities. The distinction lies in the method of signal detection: in the first setup, direct detection is employed, whereas heterodyning detects the signal within the power spectrum of the detected time domain signal. Analyzing this signal unveils insights unattainable through direct detections. In direct detections, the signal-to-noise ratio (SNR) mirrors the number of detections, thus dwindling significantly when detections are scarce. In contrast, heterodyning offers the advantage of substantially enhancing SNR through averaging.

In this paper, multiple data series of ultra-low intensity signals are collected through heterodyning and subsequently analyzed. Initially, the measurement setup is introduced, alongside foundational concepts regarding signal generation in heterodyning. Subsequently, the findings of statistical data analysis are presented and discussed.

* malz.correspondence@gmail.com

II. MEASUREMENT SETUP AND METHODOLOGY

Figure 3 illustrates the test setup used in this experiment. The experimental setup incorporates a swept source (Bridger Photonics), responsible for generating frequency sweeps (power output of approximately $3.2mW$ at $1550nm$) and initiating detection via triggering a detection board. For detection purposes, an APD-based balanced detector ("BD", Thorlabs PDB570C) with a responsivity of $R = 1A/W$ and a quantum efficiency of $\eta = 0.8$ at $1550nm$ is employed, incorporating an integrated electrical amplifier. An additional Low-Noise Amplifier (Nooelec LaNA HF) amplifies the signal to an optimal level for the ADC. The amplified analog signal is then captured through a National Instruments DAQ system (NI PXIe-1082, NI PXIe-5763). All other components within the setup adhere to standard specifications.

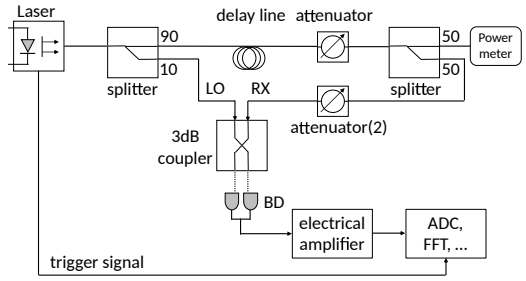

FIG. 3. Measurement Setup

The frequency transition rate of the sweep is specified at 100GHz/s, generating two linear sweeps in both directions lasting approximately 35µs each. The sampling rate is set to 500MSamples/s. To mitigate undesired noise, the optical gain of the balanced detector was minimized ($M = 2.5$), and the detection was set to the "Balanced" mode. This configuration was chosen instead of auto-balancing, as auto-balancing introduced additional noise that could not be reduced through averaging. From the recorded data, 16,384 samples were selected for each sweep ($\Delta T = 32.768\mu s$), focusing on a region where the laser was clearly locked.

The beam splitter divides the laser power into a 90:10 ratio, with the smaller portion directed as LO to the detector to ensure it remains below the detector's damage threshold. The signal path comprises an adjustable delay line and attenuator. This facilitates the fine-tuning of the overall signal delay to precisely match a frequency domain bin and pre-adjusts the signal level for monitoring purposes. Subsequently, another attenuator is employed to further decrease the signal level to achieve the detection of single photons.

The sampled signal can be mathematically represented as follows [1]:

$$i_{bd}(t) = \frac{2\eta q}{T}\sqrt{N_{LO}N_{sig}}\cos(2\pi\kappa\tau t + \phi) + i_s(t) \quad (1)$$

In Equation 1, the variable κ represents the linear chirp rate of the laser, τ corresponds to the signal delay, η denotes the quantum efficiency of the detector, q signifies the elementary charge, ϕ represents a fixed phase, and N_{sig} and N_{LO} denote the number of photons in the signal and local oscillator path during a measurement interval, respectively. The signal is subject to noise $i_s(t)$, primarily stemming from the shot noise of the local oscillator.

For an LO photon flux much larger than the signal flux, $i_s(t)$ is a Gaussian random process with zero mean and variance

$$\sigma^2(t) = \frac{2\eta q^2}{T}BN_{LO} \quad (2)$$

where T is the measurement interval and B is the sample bandwidth. The difference in optical path length $d = \tau c$ will cause a beat frequency

$$f_{beat} = \kappa\tau = \kappa\frac{d}{c} \quad (3)$$

Thus, the extraction of distance information from the detected signal in the time domain can be achieved through the utilization of a Fourier transform. As the noise is directly related to N_{LO}, a normalization of the spectrum by shot noise directly estimates the number of received photo electrons. The number of photons detected in an ideal heterodyne detection system, limited by shot noise, and subsequently normalized to a noise floor of 1, is

$$N = \frac{1}{\eta}(S - 1) \quad (4)$$

A non-ideal, real measurement system exhibits further noise, that will increase the noise floor of the system and make S smaller, when the noise floor is normalized. Additional noise can stem from the detector, for example when an APD is used. The electrical amplifier also adds additional noise. A real detector will also exhibit a non perfect overlap of the electrical fields at the detector, which results in an antenna efficiency A_{eff} lower than 1 [2]. Last but not least, losses L that can be attributed to laser phase noise and coupling losses at fiber connectors after the power meter will further diminish the Signal S. The number of photons detected in a heterodyne detection system, normalized to a noise floor of 1, therefore is

$$N = \frac{F_{ph}F_{amp}}{\eta A_{eff}L}(S - 1) \quad (5)$$

where S is the signal level in the normalized power spectrum, F_{ph} and F_{amp} are excess noise factors of the photo diode and the electrical amplifier, A_{eff} is the antenna efficiency of the detector and L are further losses.

The noise of the electrical amplifier (which strictly includes any dark noise from the detector) can be characterized as excess noise. It is determined by comparing the noise levels when the laser is active to when it is inactive:

$$F_{amp} = \frac{\sigma_{on}^2}{\sigma_{on}^2 - \sigma_{off}^2} \tag{6}$$

The excess noise of the APD is calculated as $F = M^i$, where M denotes the gain (with $M = 2.5$ at the lowest gain setting) and i represents the excess noise index, specified as 0.3 for this particular sensor, resulting in $F_{ph} = 1.32$.

Figure 4 depicts the noise in the system, which has been normalized to optical noise originating from shot noise and excess noise of the APD.

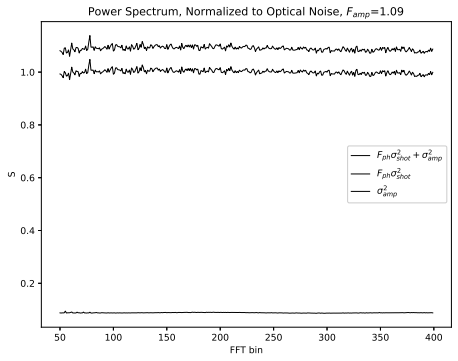

FIG. 4. Shot Noise and Noise from Electrical Amplifier

Figure 5 illustrates the normalized power spectrum in the presence of a signal.

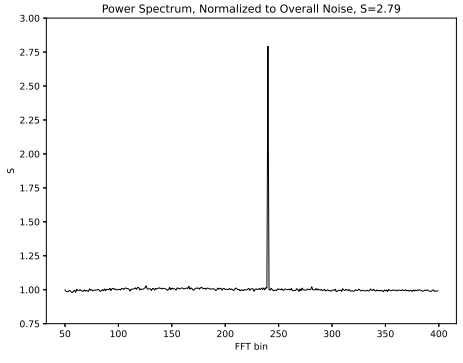

FIG. 5. Signal and Noise Floor after Normalization

When examining equation 5, it's crucial to note that all factors scaling the signal to the number of received photons do not alter the statistical behavior of S. Similarly, if, for example, an average of 5 photons per arbitrary time unit lands on a detector with a quantum efficiency of $\eta = 0.8$, then the detected average of 4 photoelectrons also adheres to Poissonian statistics.

Statistics plays a pivotal role in making heterodyning particularly intriguing for investigating the true nature of light and electromagnetic fields. A close examination of equation 1 reveals an interesting observation: the amplitude of the beat signal depends on $\sqrt{N_{LO}N_{sig}}$, where N_{LO} is a constant. The noise present in the signal, N_{sig}, thus combines with any other noise. When two statistically independent signals containing noise are combined, their variances (and hence, noise) become convoluted. Consequently, the noise observed in the beat signal is indicative of the noise present in the number of detected photoelectrons.

Two scenarios are of particular interest. The first adheres to the standard model, which follows the concept of photons. In this model, the number of photons received within a certain interval is an average, and the statistics are Poissonian. However, it has never been definitively established whether this statistical distribution is inherent to the electrical field itself, which may already be quantized, or if it arises solely from the detection process, which depends on a minimum of one photoelectron. The second scenario posits a non-quantized, relatively constant electric field, contrasting with the current paradigm of photons.

In both scenarios, the statistics observed in the beat signal would differ. When the power spectrum is normalized to a noise floor of 1, the underlying complex signal of the spectrum is Gaussian and possesses a zero mean and a variance of 0.5 in both its real and imaginary parts. If a real signal of significant magnitude ($value >> 1$) is added to this noise profile, the variance-mean ratio yields $Q = \frac{\sigma^2}{\mu} \approx 2$ when the signal is constant. In cases where the signal itself adheres to a Poissonian distribution ($\sigma^2/\mu = 1$), the variance-mean ratio approaches $Q \approx 3$ for the sum. For smaller signal values, the variance-mean ratio of the sum can be readily computed through stochastic simulation.

III. RESULTS AND DISCUSSION

The data acquired and the corresponding computations are accessible on Figshare [3]. Figure 5 illustrates the relationship between the energy in the signal path, expressed as the number of photons during a measurement interval, and the detected value in the power spectrum using the measurement setup described. This relationship accounts for excess noise and quantum efficiency but does not include considerations for antenna efficiency and additional losses.

Both graphs exhibit linearity, with fewer losses observed in the up chirp. This suggests better control of laser linearity, and consequently, linewidth and phase

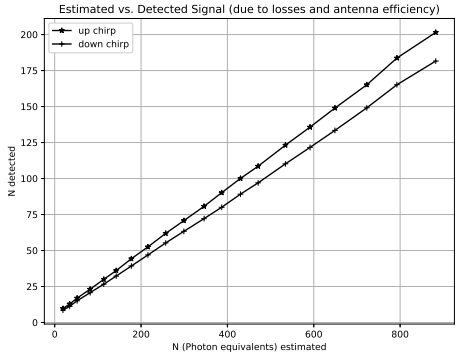

FIG. 6. Energy in Signal Path in Photon Equivalents vs. Detection before considering Antenna Efficiency and additional losses

noise, during the up chirp. However, at 0 input, a linear regression of the graphs does not yield zero detections. One possible explanation is an offset in the measured laser power of approximately 16nW. Accounting for this potential offset, Figure 7 illustrates the value of $L \cdot A_{eff}$ for different estimated input levels. The values are ≈ 0.4 and ≈ 0.35 for up and down chirp respectively.

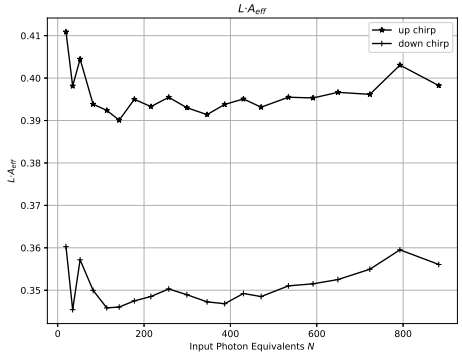

FIG. 7. $L \cdot A_{eff}$ for different estimated input levels

Excess noise of the amplifier (including detector dark noise) is $F_{amp} = 1.09$ and 1.08 for up and down chirp respectively, excess noise of the APD is, as already introduced, $M = 1.32$.

Figure 5 illustrates the variance-mean ratio for various input energy levels, with the value converging toward 2, indicating a constant signal. The slight deviation from 2 may be attributed to the relatively small number of averages taken.

Tables I and II present the results from data series with more data points, where the number of averages was significantly increased. In these cases, the variance-mean ratio of the signal closely aligns with the estimated value expected for a signal that adheres to a constant signal hypothesis.

The data unequivocally suggests that the signal of interest maintains a consistent value across all data points. To reiterate, each measurement interval comprises 16384 samples extracted from a time series of measurements conducted on a balanced detector. A single data point is then derived from the value obtained at a specific frequency of the Fourier transform of the time domain series, corresponding to a particular delay in the signal path. Particularly when the energy in the signal path is very low, the value of this data point is largely obscured by shot noise from the local oscillator and system noise. Consequently, it is impossible to infer the exact value acquired during the measurement interval of $32.768\mu s$ from a single measurement alone. Only through averaging can this value be ascertained. However, in doing so, it becomes unclear whether this averaged value represents a noisy average or if it indeed remains constant throughout each measurement interval. The statistical analysis undertaken precisely reveals that each measurement's value aligns with the average value.

Now that we have established the knowledge that the value in a single measurement corresponds with the average value, we can explore whether there is a lower threshold. Figures 9 and 10 illustrate the raw signal taken for a specific delay with a strongly attenuated signal.

The number of photon energy equivalents measured

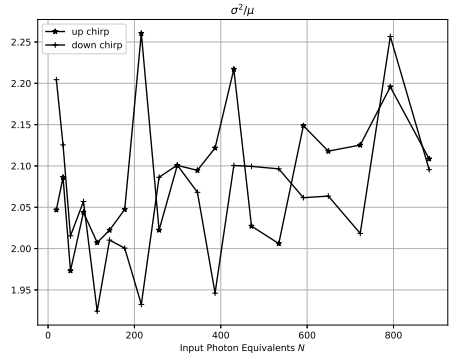

FIG. 8. Variance-mean ratio $Q = \sigma^2/\mu$ for different energy levels, with $n = 3000$ averages

TABLE I. Variance-mean ratio $Q = \sigma^2/\mu$ for different energy levels, with $n = 30000$ averages; μ: mean signal value $(S-1)$, Q_c: estimated variance-mean ratio Q for a constant signal, Q_P: estimated variance mean ratio Q in the power spectrum for a Poissonian signal distribution, Q_{meas}: Q determined from data

chirp	μ	Q_c	Q_P	Q_{meas}
up	1.63	2.61	3.61	2.52
down	1.50	2.67	3.67	2.57
up	1.15	2.87	3.87	2.77
down	1.03	2.97	3.97	2.83
up	2.10	2.48	3.48	2.37
down	1.86	2.54	3.54	2.37

TABLE II. Variance-mean ratio $Q = \sigma^2/\mu$ for different energy levels, different sensor: Thorlabs PDB480C-AC, Dataset 2 [4]; see Table I for other values

chirp	n	μ	Q_c	Q_P	Q_{meas}
up	50000	20.11	2.05	3.05	2.04
down	50000	18.05	2.05	3.05	2.07
up	50000	29.48	2.03	3.04	2.04
down	50000	26.38	2.04	3.04	2.03
up	50000	38.99	2.02	3.02	2.04
down	50000	34.90	2.03	3.03	2.02
up	41330	78.11	2.01	3.01	2.04
down	41330	70.28	2.01	3.01	2.03

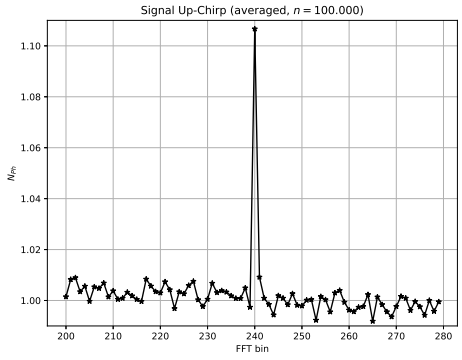

FIG. 9. Signal in Normalized Power Spectrum for Ultra-Low Intensity; Up Chirp

per interval can be determined according to Equation 5 as approximately $N \approx 0.5$ photons per measurement interval for both the up and down chirps. Consequently, the experimental outcome contradicts established notions in the photon concept: the energy measured in an interval can be fractional, can be less than 1 photon, and remains constant in each measurement instead of following a Poissonian distribution.

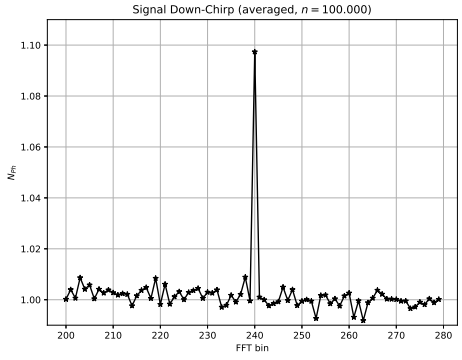

FIG. 10. Signal in Normalized Power Spectrum for Ultra-Low Intensity; Down Chirp

IV. CONCLUSIONS

In the realm of science, a theory is held to the rigorous standard of encompassing all observable phenomena within its explanatory framework. Should a theory falter in elucidating even a solitary instance, it faces the peril of being rendered invalid. The process of falsification necessitates no judgment on the correctness or fallacy of other experiments; its sole mandate is to pinpoint the deficiencies within a given model or theory. Therefore, the aim of this experiment is not to discredit the entirety of previous experiments purportedly validating the existence of photons [5–7].

However, a brief commentary on these experiments is warranted: none of them (emphasis on "none") definitively established the existence of photons. Instead, they all exhibited quantization effects in data obtained from single photon detectors, including instances of mutually exclusive detections. The concept of photons was extrapolated from the outcomes of these experiments, a conclusion reached hastily, as evidenced by heterodyning measurements. There must exist alternative explanations for the quantization and mutually exclusive detections observed in such experiments, and indeed, there are numerous possibilities. For instance, in all these experiments, a beam splitter is either treated in its idealized form or the quantization in the form of photons is presupposed at the beam splitter, resulting in circular reasoning. However, it's essential to recognize that a beam splitter, like a detector, is composed of matter. Thus, when electromagnetic fields with single-source photons (as units of energy) are utilized, the interaction of such a field differs significantly from the interaction of an attenuated, continuous laser. In the latter case, the system is in equilibrium, including the beam splitter. However, a single-photon source field interacts with a system in its initial state, leading to different dynamics. Consequently, the observed effects in these experiments likely stem from interactions between one or two electromagnetic, single-photon-source fields and the beam splitter, rather than from the existence of quantization in the field.

The data from heterodyning experiments starkly lacks any evidence of quantization and, in fact, reveals measured energy quantities smaller than those traditionally attributed to photons. Given that photons are theorized as indivisible entities and the principle of quantization is upheld within the field, the photon theory falls short in explaining these observations, rendering it falsified. This outcome is uniquely discernible through heterodyning, as it allows for the observation of energy within the pure electromagnetic field, devoid of disturbances from field-matter interactions, which can be effectively filtered out through averaging.

The effect cannot be explained by uncertainty or self-interference either. Beating only occurs when fields of different frequencies interfere, what excludes the possibility of self-interference. Furthermore, the frequency within one sweep is constantly changing, requiring that

the energy source for each time domain sample during one measurement is made of different photons. Photons can be subject to frequency broadening (increasing the length of their wave packet), but they cannot express a linear frequency sweep.

This eventually brings us to a model of the electromagnetic field that is purely semiclassical. In this model, quantization occurs at the source when energy is released into the electromagnetic field and during detection. The field itself is not quantized. Specifically, electromagnetic fields from different sources can interfere partially, even down to levels of fractional values of $h\nu$. Only the sum of these interactions is subject to quantization again at a detector. The electromagnetic field itself is not subject to postulated quantum effects.

ACKNOWLEDGMENTS

In expressing my gratitude, I extend heartfelt appreciation to Elli for her unwavering support throughout this journey. Daniel's continual encouragement has been instrumental in bolstering my resolve during the challenges encountered in the publication process. Additionally, I am indebted to Gerhard for his invaluable recommendations regarding the content and quality of the paper. Their contributions have been indispensable, and I am truly thankful for their guidance and assistance.

[1] Z. W. Barber, J. R. Dahl, T. L. Sharpe, and B. I. Erkmen, Shot noise statistics and information theory of sensitivity limits in frequency-modulated continuous-wave ladar, JOSA A **30**, 1335 (2013).

[2] A. Siegman, The antenna properties of optical heterodyne receivers, Applied optics **5**, 1588 (1966).

[3] A. Malz, Heterodyning, dataset 1 (2024), figshare (2024), `https://doi.org/10.6084/m9.figshare.24073172.v2`.

[4] A. Malz, Heterodyning, dataset 2 (2024), figshare (2024), `https://doi.org/10.6084/m9.figshare.25467538.v1`.

[5] J. Thorn, M. Neel, V. Donato, G. Bergreen, R. Davies, and M. Beck, Observing the quantum behavior of light in an undergraduate laboratory, American journal of physics **72**, 1210 (2004).

[6] C.-K. Hong, Z.-Y. Ou, and L. Mandel, Measurement of subpicosecond time intervals between two photons by interference, Physical review letters **59**, 2044 (1987).

[7] T. Legero, T. Wilk, M. Hennrich, G. Rempe, and A. Kuhn, Quantum beat of two single photons, Physical review letters **93**, 070503 (2004).